JOURNAL OF CATALYSIS **169,** 480–489 (1997)
ARTICLE NO. CA971737

Hydrogenation of Aromatics in Diesel Fuels on Pt/MCM-41 Catalysts

A. Corma,* A. Martínez,*,[1] and V. Martínez-Soria†

*Instituto de Tecnología Química, UPV-CSIC, Universidad Politécnica de Valencia, Camino de Vera s/n, 46071 Valencia, Spain; and †Departament d'Enginyería Química, Universitat de València, Doctor Moliner 50, 46100 Burjassot (València), Spain

Received November 25, 1996; revised April 14, 1997; accepted April 15, 1997

The hydrogenation activity of Pt supported on two mesoporous MCM-41 samples differing in their chemical composition has been studied by following the kinetics of the hydrogenation of naphthalene at 225–275°C reaction temperature and 5.0 MPa total pressure and by comparing the kinetic parameters obtained with Pt supported on a mesoporous amorphous silica-alumina (MSA) and other conventional supports, such as commercial amorphous silica-alumina (ASA), zeolite USY, γ-alumina, and silica. The two mesoporous MCM-41 and MSA materials having very high surface areas allowed for a better dispersion of the Pt particles, and they showed a superior overall hydrogenation activity as compared to the other supports. However, Pt/USY displayed the highest turnover (activity per exposed surface Pt), owing to the interaction of small Pt aggregates in the supercage of the zeolite with the strong Brönsted acid sites associated to framework aluminum forming electron-deficient Pt species of known enhanced activity. Moreover, both the Al-MCM-41 and USY-based catalysts presented the highest sulfur tolerance during the hydrogenation of a naphthalene feed containing 200 ppm sulfur added as dibenzothiophene. The high metal dispersion and the interaction of the small Pt clusters with the mildly acidic sites present in Al-MCM-41 may account for its high sulfur tolerance. The superior hydrogenation activity and sulfur tolerance of Pt-MCM-41 catalyst observed in the naphthalene experiments were further confirmed during the hydrogenation of a hydrotreated light cycle oil (LCO) feed containing ca 70 wt% aromatics and 400 ppm sulfur.

INTRODUCTION

As a consequence of the stringent environmental regulations directed to lower hazard emissions from vehicle exhausts, together with the growing demand for high quality diesel fuels, hydrotreating processes are playing an important role in the modern refinery strategies. New diesel fuel specifications will include a reduction of sulfur to 0.05 wt% maximum and of aromatics content, while the cetane number will be set to a minimum value of 40 (1–4). Although the role of aromatics in particulate emissions of diesel fuels has not been at present clearly established, it has been shown that a reduction of the aromatics content has a positive effect on the cetane number (5, 6). Therefore, there is considerable interest in developing new catalysts and processes for aromatics saturation with improved activity and stability at moderate temperatures.

Conventional hydrotreating catalysts containing sulfided mixed oxides (NiMo, NiW, CoMo) can only accomplish moderate levels of aromatics saturation under typical hydrotreating conditions in a single-stage operation (1–3, 7). With these systems, increasing operation severity (temperature and H_2 pressure) do not result in deep levels of aromatics saturation because of thermodynamic limitations. In this sense, noble-metal based catalysts are preferred for deep aromatics saturation (1–4) since they can work at lower temperatures, thus avoiding the thermodynamic constraints encountered with the sulfided oxides. The main drawback of noble-metal hydrogenation catalysts is that they are readily poisoned by small amounts of sulfur and nitrogen organic compounds present in the feed (8, 9), and consequently, they are used in the second reactor of a dual-stage process, where the feed is severely pretreated in the first reactor to reduce the level of heteroatoms up to a few ppm. Furthermore, the sulfur and nitrogen tolerance of noble metals (Pt, Pd) were seen to strongly improve when they are supported on a zeolite (1–3). Thus, Pt(Pd)-USY catalysts are able to maintain high hydrogenation activities with feeds containing several hundred ppm of sulfur under more thermodynamically favorable conditions than those typically used in a single-stage hydrotreating. Indeed, the nature of the noble metal, the presence of a secondary metal as promoter, and the type and characteristics of the support are all important parameters affecting the hydrogenation activity and sulfur tolerance of noble metal-based catalysts (10–15). In this respect, we have recently shown (16) that NiMo-supported on (Al)-MCM-41 material, having a hexagonal arrangement of uniform mesopores and very high surface area (17), is more active than conventional NiMo-alumina and NiMo-USY catalysts for mild hydrotreating of vacuum gas oil.

The mesoporous aluminosilicate MCM-41 has also been shown to be a suitable support for preparing noble metal-based catalysts. Thus, Pt and/or Pd containing Al-MCM-41 was already claimed as a catalyst for the low temperature

[1] To whom correspondence should be addressed. E-mail: amart@itq.upv.es.

0021-9517/97 $25.00

hydrogenation of benzene (18) and for the hydrogenation of aromatics in diesel and kerosene feeds (19). On the other hand, Reddy and Song found that the use of aluminum isopropoxide as the Al source during the synthesis of Al-MCM-41 led to samples presenting a higher Al incorporation, better crystallinity, and higher catalytic activity than those prepared from pseudo-bohemite (20). Moreover, it was also shown that Pt supported on Al-MCM-41 prepared from aluminum isopropoxide is highly active for aromatics hydrogenation (21). The same authors have also reported that Pt and Pd supported on Al-MCM-41 are more active for the hydrogenation of naphthalene at low temperatures as compared to alumina and titania supported catalysts (22).

In this work we have further investigated the catalytic performance of Pt-supported MCM-41 catalysts for the hydrogenation of aromatics. For this purpose, we firstly studied the hydrogenation of naphthalene as a model compound in a batch reactor at 225–275°C reaction temperature and 5.0 MPa total pressure on two MCM-41 catalysts differing in their chemical composition. The results obtained with Pt/MCM-41 were then compared with those obtained using different supports, i.e., a mesoporous silica-alumina (MSA) synthesized by Eni (23), a commercial amorphous silica-alumina (ASA, 25 wt% alumina), an ultrastable Y zeolite (USY), γ-Al_2O_3, and SiO_2, all of them having the same Pt content. The sulfur tolerance of these catalysts was studied by adding 200 ppm(w) of dibenzothiophene (DBT) to the naphthalene feed. In the second part of the work, we have carried out the hydrogenation of a light cycle oil (LCO) feedstock containing ca 70 wt% aromatics and 1600 ppm sulfur previously hydrotreated to reduce the sulfur level to 400 ppm. This study was performed in a continuous fixed-bed reaction system at 300–350°C and 5.0 MPa.

EXPERIMENTAL

Preparation and Characterization of Catalysts

A pure silica and a Al-containing (Si/Al = 16) MCM-41 samples (denoted as MC-1 and MC-2, respectively), were synthesized from Aerosil as silica source and Al_2O_3 $4H_2O$ as the alumina source (in the case of MC-2), trimethylammonium hydroxide (TMAOH), and hexadecyltrimethylammonium (CTMA) bromide as the surfactant template, following the procedure reported in Ref. (24). Thus, gels of the following molar composition:

MC-1) 0.15 CTMA: 24.3 H_2O: 0.26 TMAOH: SiO_2

MC-2) 0.40 CTMA: 24.3 H_2O: 0.26 TMAOH: 0.036 Al_2O_3: SiO_2

were crystallized in teflon-lined stainless steel autoclaves at 135°C in static conditions, and then the solids were washed, filtered, dried at 60°C, calcined in nitrogen flow (150 cm^3/min) at 540°C for 1 h, and, finally, calcined in air (150 cm^3/min) at the same temperature for 6 h.

For comparison purposes, the following materials were also used as supports: an amorphous mesoporous silica-alumina (MSA, Si/Al = 100) supplied by Enichem and exhibiting a narrow pore size distribution (23); a commercially available amorphous silica-alumina (ASA) (Crossfield, 25 wt% alumina); a USY zeolite (CBV760, PQ Corp., $a_0 = 2.426$ nm); γ-Al_2O_3 (Merck); and SiO_2 (BASF).

All these supports were impregnated with the required amount of hexachloroplatinic acid in a 0.2 *N* HCl aqueous solution (3 ml/g solid) and the solvent evaporated in a rotatory evaporator, dried at 100°C and, finally, calcined at 500°C for 3 h. The nominal Pt content in all catalysts was 0.5 wt% and 1 wt% for the hydrogenation of naphthalene and LCO, respectively.

X-ray diffraction (Philips PW 1830, CuKα radiation) was used to ascertain the structure and pore size of the mesoporous MCM-41 materials. The textural properties of the different supports were evaluated from the nitrogen adsorption–desorption isotherms at 77 K in a ASAP-2000 apparatus (Micromeritics). Infrared spectroscopy (Nicolet 710 FTIR equipment) with adsorption–desorption of pyridine was used to measure the acidity of MCM-41 (sample MC-2), MSA, ASA, and USY catalysts. The details of the experimental conditions used for the IR-pyridine experiments can be found in Ref. (25). Chemisorption of hydrogen was performed at 20°C using the pulse flow method in a Chemisorb 2700 (Micromeritics) apparatus. Before the chemisorption measurements the catalysts were reduced in H_2 at 450°C for 2 h, followed by cleaning of the surface at the same temperature for 1 h in N_2 flow.

Reaction System and Procedure

The kinetic experiments for naphthalene hydrogenation were performed in a 0.5 L batch stirred reactor (Autoclave Engineers, Inc.) equipped with inlet and outlet valves for adding or removing gases, and a liquid sample valve attached to a dip tube extending to the bottom of the reactor in order to sample products at different reaction times. The system includes a reactant loader for good zero-time determination. In this way, 1 g of prereduced catalyst is introduced into the reactor and heated up to the desired reaction temperature in hydrogen atmosphere. Then, 100 g of a 10 wt% solution of naphthalene (Merck, >98% purity) dissolved in *n*-decane (Arcross, >99.5% purity) are added from the loader to the reactor, and the system is pressurized with H_2 at the operating pressure. For the determination of sulfur tolerance of Pt-supported catalysts, 200 ppm(w) of sulfur as dibenzothiophene (DBT) were added to the naphthalene solution. The hydrogenation experiments were carried out at 225–275°C reaction temperature and 5.0 MPa total pressure. The catalysts were previously reduced at

450°C for 1 h in H_2 flow (250 cm^3 min^{-1}) at atmospheric pressure in a fixed bed system, and immediately transferred to the batch reactor for the kinetic measurements. In order to determine the possible influence of external mass transfer limitations we performed preliminary hydrogenation experiments at 275°C and 5.0 MPa in which we varied the stirring speed from 200 to 2000 rpm while keeping constant the rest of parameters. It was seen that the pseudo-first-order kinetic rate constant, first, increased from 200 to 500 rpm and, then, hardly changed in the range of 500–2000 rpm. According to these results, we selected an agitation rate of 1000 rpm for the kinetic experiments. Similarly, we did not observe significant changes in the reaction rate when using catalyst particles of 0.1–0.25 mm or 0.59–0.84 mm diameter, so we used the smaller particles to be sure that in our experiments the reaction was not controlled by intraparticle mass resistance. The mass balance in all experiments was above 98% of the initial reaction mass. The products were analyzed by GC (Varian 3400) equipped with a FID detector and a capillary column (Supelco SPB-1, 30-m length).

Hydrogenation of a hydrotreated LCO was conducted in a fixed-bed stainless steel tubular reactor at 300 and 350°C reaction temperature, 5.0 MPa total pressure, WHSV = 4 h^{-1}, and a H_2/feed ratio of 1000 stp. Under these conditions some deactivation of the catalysts was observed during the first 3–5 h onstream. The catalytic data reported for these flow reactor studies correspond to reaction times above 6 h onstream, for which a stationary state behavior was achieved. The total aromatics content and aromatics distribution in the feed and hydrogenated products were determined by gas chromatography in a GC Varian 3400 apparatus equipped with a FID and a capillary column (Petrocol DH-100, fused silica, 100-m length). Identification of the main aromatic components in the LCO feed and the hydrogenated products was carried out by mass spectrometry in a GC-MS (Varian 3400) equipped with the same kind of capillary column described above in order to obtain the same retention times for each component in the two GC analysis. All the catalysts were previously reduced "in situ" at 400°C for 2 h at atmospheric pressure in hydrogen flow. Hydrotreatment of the original LCO was carried out with a commercial CoMo/alumina catalyst (TK-550, Haldor–Topsoe) at 400°C, 3.0 MPa, WHSV = 0.3 h^{-1}, and H_2/feed ratio of 1000 stp in order to reduce the sulfur content.

RESULTS AND DISCUSSION

Characterization of Catalysts

The X-ray diffractograms of the calcined MCM-41 samples (Fig. 1) show the typical low angle reflection at about $2\Theta = 2^\circ$ characteristic of this material (17). In agreement with previous works (26, 27) a more well-defined XRD pattern corresponding to an hexagonal arrangement of pores is observed for the siliceous MC-1 sample (Fig. 1a) as compared to the aluminosilicate MC-2 sample (Fig. 1b). The pore size calculated from the position of the (100) XRD peak is slightly higher for the Al-containing MC-2 sample (42.6 Å) as compared to the pure silica MC-1 sample (37.3 Å). Moreover, impregnation of Pt did not change appreciably the pore size of MCM-41 (Fig. 1c).

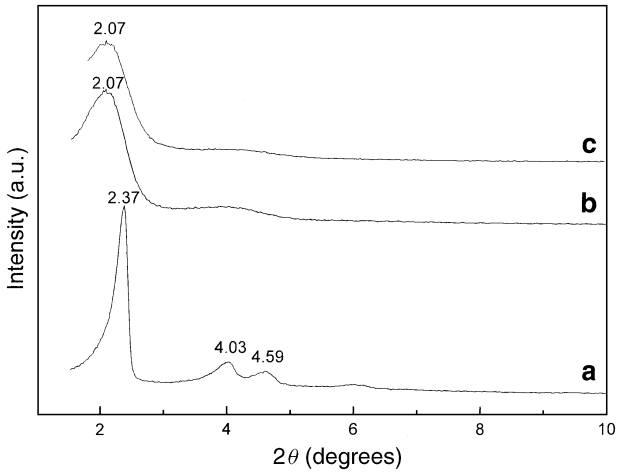

FIG. 1. XRD patterns of calcined MCM-41 samples: (a) MC-1; (b) MC-2; and (c) Pt/MC-2.

The physicochemical and textural properties of the different supports are given in Table 1. The two MCM-41 samples show, together with the mesoporous silica-alumina (MSA), the highest surface area. The total pore volume is

TABLE 1

Chemical Composition and Textural Properties of MCM-41 Materials and Different Supports Determined by Nitrogen Adsorption–Desorption Experiments

Support	Bulk SiO_2/Al_2O_3 ratio	BET surface area (m^2 g^{-1}) Total	BET surface area (m^2 g^{-1}) Micropore	Pore volume (cm^3 g^{-1}) Total	Pore volume (cm^3 g^{-1}) Micropore	APD[a] (Å)
MC-1	∞	1046	—	0.91	—	27.7
Pt/MC-1	∞	989	—	0.82	—	nd[c]
MC-2	32	834	—	1.03	—	30.9
Pt/MC-2	32	694	—	0.73	—	nd
MSA	100	750	—	—	—	nd
ASA	3	268	21	0.31	0.01	46.0
USY	56[b]	551	362	0.41	0.18	21.0
γ-Al_2O_3	100	122	—	0.18	—	nd
SiO_2	0	137	6	0.74	0	nd

[a] Average pore diameter as measured from Ar adsorption–desorption isotherms at 87 K and using the Horvath–Kawazoe equation (45).
[b] Framework Si/Al ratio = 62.2 (a_0 = 24.26 Å).
[c] nd = not determined.

TABLE 2

Acidity of the Different Al-Containing Supports Used as Measured by IR Spectroscopy with Adsorption of Pyridine and Desorption at Different Temperatures

	Acidity (μmol pyridine/g catalyst)[a]					
	Brönsted			Lewis		
Support	150°C	250°C	350°C	150°C	250°C	350°C
MC-2	19	6	0	58	39	22
MSA	17	5	0	53	42	28
ASA	22	10	2	60	38	22
USY	—	37	15	—	20	13

[a] Calculated using the extinction coefficients given in Ref. (46).

TABLE 3

Results of H_2 Chemisorption Experiments on the Different Pt-Supported Catalysts,[a] after Reduction with Hydrogen at 450°C for 2 h

Catalyst	H_{irr}/Pt (%)	Area (m^2 Pt/g cat)	d (Å)
Pt/MC-1	82	1.12	12.4
Pt/MC-2	68	0.94	14.9
Pt/MSA	85	1.18	11.9
Pt/ASA	19	0.26	53.8
Pt/USY	13	0.18	77.2
Pt/γ-Al_2O_3	77	1.06	13.2
Pt/SiO_2	6	0.08	175.0

[a] Nominal Pt content = 0.5 wt%.

also higher for the MCM-41 samples. Contrary to MCM-41 and MSA supports, the USY zeolite presents most of its pores in the micropore range, although some mesoporosity, probably created during the hydrothermal treatments, is also observed in the zeolite. As shown in Table 1, both the BET surface area and pore volume of MCM-41 slightly decrease after the impregnation of Pt, the decrease being more significant in the case of the Al-containing Pt/MC-2 catalyst. Anyway, the surface area and pore volume of the Pt-containing MCM-41 samples are still very high, which, besides the XRD data, indicate that most of the MCM-41 structure was preserved after the impregnation step.

The acidity results measured by IR-pyridine at different desorption temperatures are given in Table 2. USY zeolite presents the higher Brönsted acidity, both in terms of acid site density and acid strength. On the other hand, the Al-containing MCM-41 (sample MC-2), the MSA, and the commercial amorphous silica-alumina (ASA) show a similar Brönsted acidity, with most of the sites being of weak-medium strength. Indeed, no Brönsted acid sites are practically observed on these supports at 350°C desorption temperature.

The hydrogen chemisorption results obtained for the Pt/supported catalysts (0.5 wt% nominal Pt content) are shown in Table 3. It is seen there that the amount of hydrogen irreversibly adsorbed, H_{irr}/Pt, after reduction with hydrogen at 450°C for 2 h, is higher for the mesoporous MCM-41 and MSA supports, suggesting a fairly high Pt dispersion as a consequence of the high surface area of these materials. Accordingly, a higher Pt dispersion is also observed for the siliceous MCM-41 sample (Pt/MC-1) as compared the Al-containing Pt/MC-2 catalyst, which may be ascribed to the significantly higher surface area of the former sample (Table 1). A high dispersion (77%) is also observed for Pt/γ-Al_2O_3, probably due to a strong interaction of the metal with the alumina surface, preventing sintering of the Pt particles during the thermal treatments. However, relatively low metal dispersions (less than 20%) are observed for Pt/ASA and Pt/USY catalysts. In the case of Pt/USY, the low Pt dispersion might be attributed to a bimodal Pt distribution, with very small Pt clusters located inside the zeolite cavities and large Pt aggregates predominanting on the external surface. This aspect will be further discussed along the work. The lowest hydrogen uptake was observed for Pt supported on silica (H_{irr}/Pt = 0.06). Probably, the low interaction of the metal with the silica surface favors sintering of the metal at the reduction temperature used, producing the formation of larger metal aggregates and lowering the number of exposed surface metal atoms.

Kinetics of Naphthalene Hydrogenation on Pt-Supported Catalysts

The general reaction scheme proposed for the hydrogenation of naphthalene is presented in Fig. 2. The hydrogenation occurs in a sequential manner, with the rate of tetraline hydrogenation being of an order of magnitude less than that of naphthalene hydrogenation (29). In our case, tetraline was the major product under the relatively mild operating conditions used in this work (P = 5.0 MPa, 225°C ≤ T ≤ 275°C). Only at high conversions the hydrogenation of tetraline into *cis*- and *trans*-decaline occurred at a significant extent. At the highest temperature studied (275°C) and at high conversions a small amount (less than 0.1 wt%) of cracking and isomerization products, such as

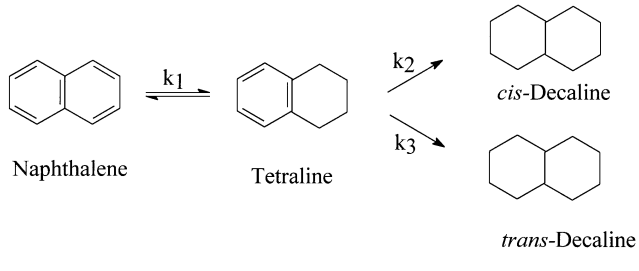

FIG. 2. General reaction scheme for the hydrogenation of naphthalene.

methylindanes, alkylbenzenes, and alkylcyclohexanes were also detected in the reaction products. The conversion-time curves obtained at different reaction temperatures on the two Pt/MCM-41 catalysts are shown in Figs. 3a–b. As an example, the selectivity to tetraline and decalines obtained at the three temperatures studied is also presented in Fig. 4 as a function of naphthalene conversion for the Pt/MC-1 sample. It can be seen that the selectivity pattern of the catalyst does not depend on the reaction temperature, at least in the range studied here, but it depends only on naphthalene conversion. Furthermore, Fig. 4 also shows that the hydrogenation of the second ring only occurs to a significant extent at very high conversions, clearly showing the secondary character of decaline, in agreement with the reaction scheme presented in Fig. 2. Similar trends were also observed for noble metal Pt and Pd catalysts supported on alumina and titania during the low temperature (200°C) hydrogenation of naphthalene (28).

According to the reaction scheme in Fig. 2, the hydrogenation of naphthalene to tetraline is a reversible reaction, while the dehydrogenation rates of decalines are negligible (29). However, in the range of temperatures used in this work the equilibrium concentration of naphthalene is negligible (2, 30) and the formation of tetraline can be considered as an irreversible process. Taking this into account, and in order to determine the kinetic rate constant for the process, and to be able to compare the activity of the different catalysts on the bases of this parameter, we have considered that the system can follow a first-order kinetic equation with respect to the hydrocarbon reactant, which after integration results in the equation

$$-\ln(1 - X) = k_1 t.$$

When this equation was fitted with the experimental results obtained for the different catalysts, Figs. 5 and 6 show that the above assumption is adequate, in agreement with previous published results (2, 12, 28, 31, 32).

As shown in Fig. 5, the catalyst based on the pure silica MCM-41 (sample Pt/MC-1) is more active in the whole range of temperatures than the Al-containing Pt/MC-2 sample. The higher surface area and better Pt dispersion obtained with Pt/MC-1 (Tables 1 and 3) can be responsible for its higher hydrogenation activity.

The pseudo-first-order rate constants for the hydrogenation of naphthalene, k_1, obtained at the three temperatures studied are given in Table 4. The corresponding apparent activation energies calculated from the Arrhenius plot of the rate constants (Fig. 8) are also included in Table 4. At the lower temperature, Pt/USY and Pt/MC-1 catalysts show the highest hydrogenation activity, while Pt/SiO_2 is the less active catalyst. However, at 275°C the mesoporous Pt/MSA and Pt/MC-1 catalysts show their superior hydrogenation activity. When the activity of the different catalysts is analyzed, one would be tempted to correlate, in a first approximation, the hydrogenation activity with the metal dispersion, or what is equivalent, with the metallic area calculated from the H_2 chemisorption measurements. Thus, when the pseudo-first-order rate constant obtained at 225°C reaction

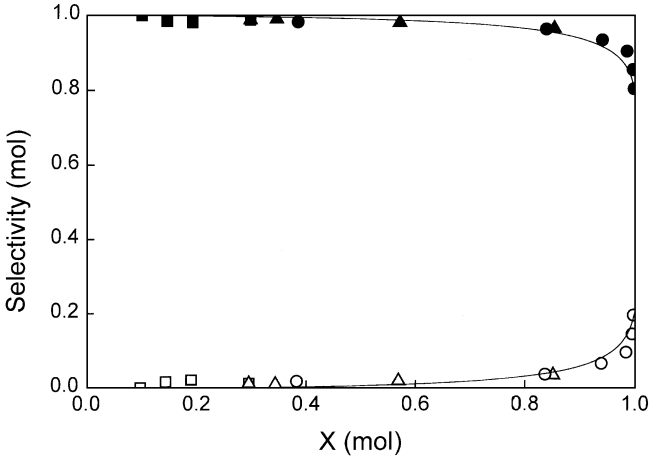

FIG. 4. Selectivity to tetraline (filled symbols) and decalines (open symbols) as a function of naphthalene conversion obtained on Pt/MC-1 catalyst at different reaction temperatures: 225°C (■); 250°C (▲); and 275°C (●).

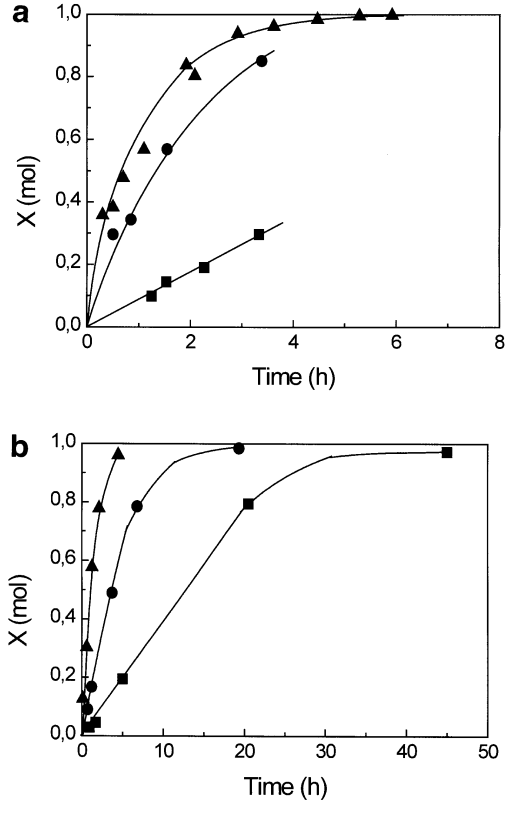

FIG. 3. Kinetics of naphthalene hydrogenation on Pt/MC-1 (a) and Pt/MC-2 (b) catalysts at different temperatures: 225°C (■); 250°C (●); and 275°C (▲).

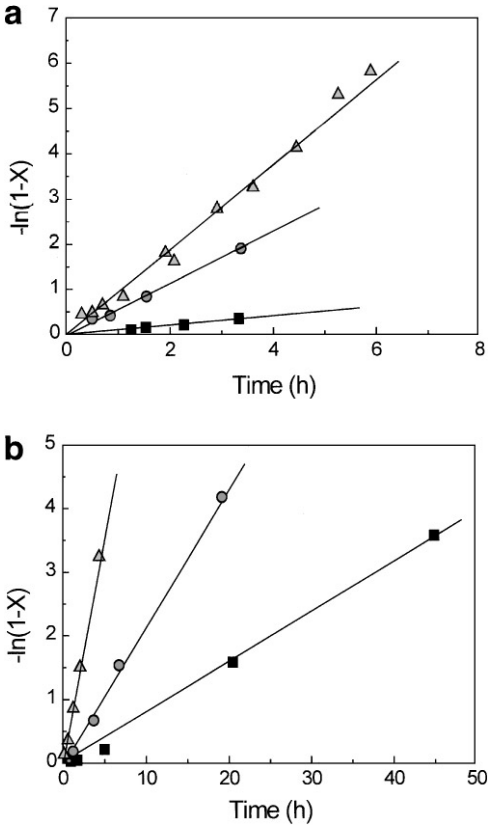

FIG. 5. Pseudo-first-order kinetic plots for naphthalene hydrogenation on Pt/MC-1 (a) and Pt/MC-2 (b) catalysts at 225°C (■); 250°C (●); and 275°C (▲) reaction temperature.

temperature (Table 4) is plotted against the area of the metallic phase (Table 3), a fairly good linear correlation is obtained for all catalysts except for Pt/USY, which displays an anomalous high hydrogenation activity (Fig. 7) despite its relatively low metallic area (and Pt dispersion). Indeed, a very high activity for the hydrogenation of naphthalene on a Pt/HY catalyst having very large (ca 170 nm) metal particle size has been recently reported by Smittz *et al.* (33). The high activity of the zeolite-based catalyst, in comparison with the other supports, might be explained, considering the formation of a bidisperse metallic phase, with most of the reaction occurring on small Pt clusters of ca 1-nm size fitting in the supercages of the Y zeolite (33). Then, the large Pt aggregates on the external surface of the zeolite crystals could explain the low H_2 uptake obtained for this catalyst (Table 3) (34, 35). Such small Pt clusters would be greatly influenced by the zeolite lattice, giving rise to the formation of electron-deficient Pt species by electron transfer from the metal to the zeolite acid centers, and would exhibit an enhanced catalytic activity towards hydrogenation reactions, as is well reported in the literature (36).

The apparent activation energies reported in Table 4 fall in the range of 95–115 KJ/mol for most of the catalysts studied, which is in close agreement with previously published data (37) for the hydrogenation of the first ring of naphthalene on metal sulfide catalysts. This value does

TABLE 4

Pseudo-First-Order Kinetic Rate Constants and Activation Energies for the Hydrogenation of Naphthalene (k_1) Obtained on the Different Pt-Supported Catalysts

Catalyst	k_1 (h^{-1}) 225°C	250°C	275°C	E_{act} (KJ/mol)
Pt/MC-1	0.114	0.556	0.911	95.2
Pt/MC-2	0.082	0.221	0.710	97.9
Pt/MSA	0.071	0.440	1.069	116.9
Pt/ASA	0.035	0.127	0.589	128.6
Pt/USY	0.138	0.352	0.554	63.5
Pt/γ-alumina	0.065	0.245	0.659	105.4
Pt/SiO_2	0.013	0.062	0.129	104.8

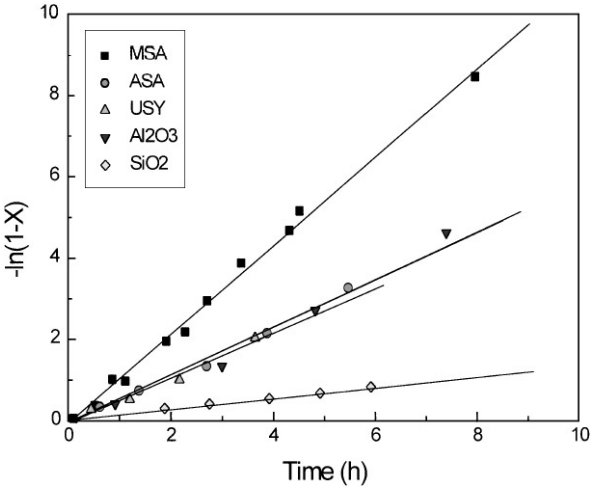

FIG. 6. Pseudo-first-order kinetic plots for naphthalene hydrogenation on different Pt-supported catalysts at 275°C reaction temperature.

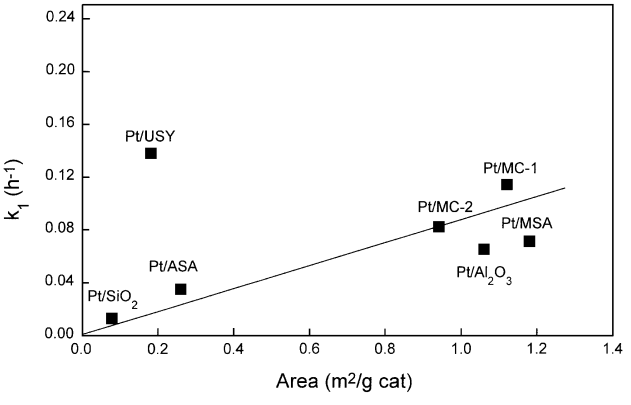

FIG. 7. Pseudo-first-order kinetic rate constant (at 225°C) for the hydrogenation of naphthalene, k_1, as a function of the metallic area of the different Pt-supported catalysts.

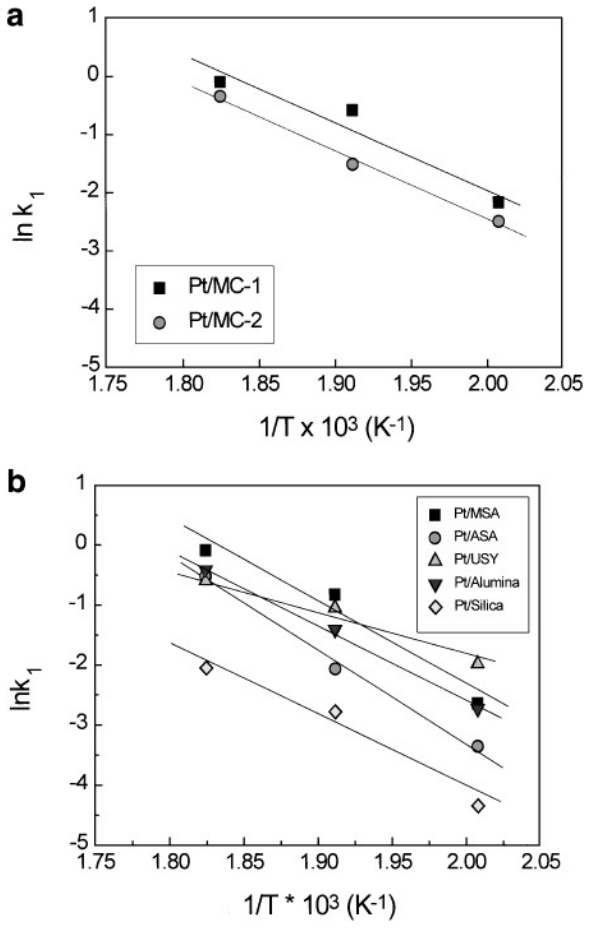

FIG. 8. Arrhenius plots for hydrogenation of naphthalene on the two Pt/MCM-41 (a) and the rest of catalysts (b) studied.

not vary much with the nature of the support, except for Pt/USY, which shows a relatively low apparent activation energy of ca 65 KJ/mol (Table 4). This is probably due to a stronger adsorption of the aromatic compound on the Brönsted acid sites of the zeolite.

The turnover frequency (TOF) of the different Pt-supported catalysts, calculated from the pseudo-first-order rate constants given in Table 4 and the number of exposed surface metal atoms derived from the H_2 chemisorption data in Table 3, are given in Table 5. It can be seen there that the activity per exposed surface platinum clearly depends on the nature of the support. Higher TOF are obtained for the most acidic Pt/USY catalyst, especially at lower reaction temperatures. Increased turnover frequencies displayed by more acidic supports have also been observed during the hydrogenation of benzene and toluene on different Pt-supported systems (10, 11, 38, 39). This fact has been explained considering an additional contribution to the overall hydrogenation rate of spilled-over hydrogen from the metal to the aromatic ring adsorbed on the acid sites of the support. On the other hand, the mesoporous

TABLE 5

Turnover Frequencies (TOF) for Hydrogenation of Naphthalene on Different Pt-Supported Catalysts

Catalyst	TOF (s^{-1}) 225°C	250°C	275°C
Pt/MC-1	1.17	5.70	9.38
Pt/MC-2	1.02	2.73	8.83
Pt/MSA	0.70	4.38	10.63
Pt/ASA	1.56	5.63	26.25
Pt/USY	8.98	22.89	36.09
Pt/γ-alumina	0.70	2.66	7.27
Pt/SiO_2	1.80	8.75	18.20

MCM-41 and MSA materials show TOF similar to that of γ-alumina, which as shown in Table 3 were the supports presenting a higher hydrogen uptake, and presumably, a higher metal-support interfacial area. Moreover, results of Table 5 suggest that the acidity of the support cannot be the only parameter to explain the specific hydrogenation activity of the catalysts, since both MCM-41 based catalysts, one of them having no Brönsted acid sites (MC-1), show similar turnover frequencies for naphthalene hydrogenation. Therefore, other factors related to the dispersion and state of the metal and the location of metal particles, which will depend on the pore geometry of the support, might also contribute to the observed specific hydrogenation rates.

The rate constants for the hydrogenation of tetraline into *cis*- and *trans*-decaline, $k_2 + k_3$, calculated assuming an irreversible pseudo-first-order consecutive reaction, and the product selectivity defined as the ratio $k_1/(k_2 + k_3)$, obtained at 275°C reaction temperature are presented in Table 6. The hydrogenation rates for the second ring of naphthalene are, in agreement with previous results (29), one order of magnitude lower than the hydrogenation rates of naphthalene to tetraline. At this temperature, the pseudo-first-order rate constants for tetraline hydrogenation obtained on the different catalysts follow

TABLE 6

Rate of Hydrogenation of Tetraline to *cis*- and *trans*-decaline ($k_2 + k_3$), and Relative Hydrogenation Rates for the First and Second Rings of Naphthalene, $k_1/(k_2 + k_3)$, Obtained at 275°C on Pt-Supported Catalysts

Catalyst	$(k_2 + k_3) \times 10^2$ (h^{-1})	$k_1/(k_2 + k_3)$ ratio
Pt/MC-1	2.6	35
Pt/MC-2	2.1	34
Pt/MSA	4.9	22
Pt/ASA	1.9	31
Pt/USY	1.9	29
Pt/γ-alumina	2.1	31
Pt/SiO_2	0.6	18

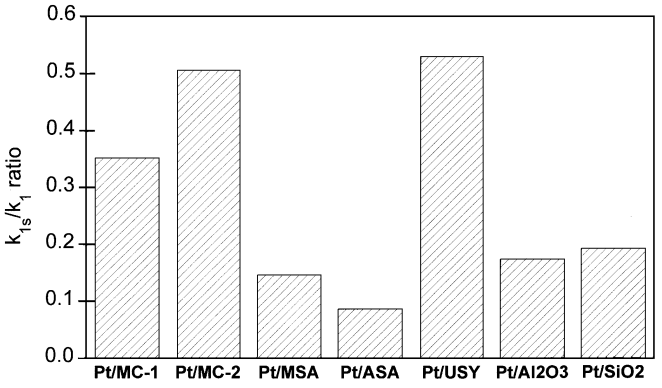

FIG. 9. Relative hydrogenation activity at 275°C of Pt-supported catalysts after addition of 200 ppm sulfur to the naphthalene feed.

the same trend previously found for the hydrogenation of the first ring of naphthalene (Table 4), i.e., MSA > MC-1 > MC-2 = γ-alumina > ASA = USY > SiO_2. On the other hand, Pt supported on the mesoporous MSA and on silica give a higher selectivity towards the hydrogenation of the second ring of naphthalene, as can be seen from the ratio between the first, k_1, and second hydrogenations, $K_2 + K_3$. Pt/MCM-41 catalysts show similar selectivity pattern to Pt supported on amorphous silica-alumina, USY, and γ-alumina.

Sulfur Resistance of Pt-Supported Catalysts

Since sulfur tolerance is an important aspect of noble metal hydrogenation catalysts, we have studied here the activity of the different Pt-supported catalysts for hydrogenation of naphthalene in the presence of 200 ppm sulfur, added as dibenzothiophene (DBT) to the naphthalene solution. The relative decrease of the pseudo-first-order rate constants after the addition of sulfur at 275°C reaction temperature is shown in Fig. 9. It can be seen that the Al-containing Pt/MCM-41 (sample Pt/MC-2) and Pt/USY are the most stable catalysts towards poisoning by sulfur under the reaction conditions used here.

The high sulfur tolerance of zeolite-based Pt catalysts is believed to arise from the formation of electron-deficient Pt particles, Pt^{n+}, upon interaction of the reduced metal with the Brönsted acid sites of the zeolite, which in turn lowers the strength of the S–Pt bond (35, 36, 40–43). Taking into account the low metal dispersion in our Pt/USY catalyst (Table 3), the high thioresistance obtained for this system might also be attributed to the formation of small Pt clusters in the supercages of the zeolite that, as discussed above, could be responsible for its high intrinsic activity. Moreover, the higher sulfur resistance of Pt/MC-2 with respect to Pt/MC-1 may also be ascribed to the presence of Brönsted acid sites in the Al-containing MCM-41 sample (MC-2). However, the acidity of the support cannot by itself explain the results presented in Fig. 9, since the Al-MCM-41, MSA, and ASA supports having similar acidity (Table 2) present quite different sulfur tolerances. Moreover, the Al-free Pt/MC-1 catalyst does not possess Brönsted acidity but it shows a relatively high resistance to sulfur poisoning. These results suggest again that not only the intrinsic hydrogenation activity but also the sulfur resistance of Pt-based catalysts is a complex function of the metal-support properties (14).

Hydrogenation of Light Cycle Oil (LCO) Feed

LCO is a by-product of fluid catalytic cracking (FCC) units which has poor blending properties for diesel fuel owing to its very high aromatics content (about 70 wt%) and high levels of S and N compounds. However, due to the increasing demand for high quality diesel fuel, upgrading of the LCO fraction would be necessary if LCO is to be used as a diesel blending component.

Here we have studied the hydrogenation performance of Pt supported on the mesoporous MCM-41 and amorphous silica-alumina supports, as well as of the Pt/USY catalyst, using a LCO feed obtained by distillation of a FCC liquid product. Due to the high sulfur content of LCO (usually 1–2 wt%), noble metal catalysts have to be used in a dual-stage hydrogenation process, where the feed has been previously hydrotreated to reduce the sulfur content. Therefore, we have hydrotreated the LCO feed using a commercial CoMo/alumina hydrotreating catalyst (TK-550 from Haldor–Topsoe) before performing the hydrogenation experiments with the different Pt-based catalysts. The characteristics of the untreated and hydrotreated LCO (LCO-HT) are given in Table 7. It can be seen that the

TABLE 7

Properties of the LCO Feed before and after Hydrotreating with a Commercial CoMo/Alumina Catalyst

	LCO	LCO-HT
Sulfur content (ppm)	1600	400
Nitrogen (ppm)	643	480
Density at 15°C (g cm^{-3})	0.9174	—
Distillation curve:		
IBP	64.3	57.8
5%	172.9	146.9
10%	205.8	177.1
30%	244.4	227.8
50%	270.8	253.5
70%	306.0	288.5
90%	349.4	336.7
95%	369.9	361.1
FBP	467.2	451.5
Aromatics content (wt%):		
Mono-	20.7	24.0
Di-	36.3	32.4
Tri+	13.6	11.6
Total	70.6	68.0

TABLE 8

Results of the Hydrogenation of a Hydrotreated LCO Feed (LCO-HT) at 300 and 350°C Reaction Temperature on the Different Pt-Supported Catalysts (1 wt% Pt)

	Pt/MC-2		Pt/MSA		Pt/ASA		Pt/USY	
	300°C	350°C	300°C	350°C	300°C	350°C	300°C	350°C
Total aromatics reduction (%)	40.3	46.2	32.1	45.4	10.9	22.8	23.4	35.7
Aromatics distribution (wt%):								
Mono-	19.8	20.4	20.9	21.4	23.1	22.3	22.4	32.7
Di-	16.3	13.5	20.5	11.7	28.0	22.9	22.9	10.4
Tri+	4.5	2.7	4.8	4.0	9.5	7.3	6.8	0.6
Total	40.6	36.6	46.2	37.1	60.6	52.5	52.1	43.7

sulfur content was reduced from 1600 to 400 ppm and that, besides sulfur removal, a partial hydrocracking also occurred during the hydrotreatment. Moreover, only a slight reduction in total aromatics content from 70.6% to 68.0% was achieved during the feed pretreatment, with the distribution of aromatics shifted towards the monoaromatics fraction (from 20.7% to 24.0%) as a consequence of the easier hydrogenation of polyaromatics, as compared to the more refractory monoaromatics.

The results of the hydrogenation of the hydrotreated LCO feed on the different Pt-catalysts at two reaction temperatures are presented in Table 8. It can be observed that the Al-containing Pt/MCM-41 catalyst (Pt/MC-2) produces the highest aromatics reduction of LCO at the two temperatures studied, and especially at the lowest temperature (300°C), the difference between Pt/MCM-41 and the rest of catalysts is more evident. The catalyst based on the mesoporous amorphous silica-alumina (MSA) also presents a relatively high aromatics reduction in LCO, compared to Pt supported on a conventional silica-alumina (ASA) and a USY zeolite. No significant hydrocracking of the LCO feed was observed at the two temperatures studied for the catalysts investigated.

The results obtained using the LCO feed confirmed the higher hydrogenation activities observed for the MCM-41 and MSA mesoporous materials during the hydrogenation of naphthalene in the absence of sulfur compounds. However, it appears that the mesoporous MSA material performs much better and the USY based catalyst performs much poorer with the LCO feed, in comparison with the experiments of hydrogenation of naphthalene in the presence of 200 ppm sulfur. This fact may be associated with the relatively high concentration of nitrogen compounds still present in the hydrotreated LCO feed (Table 7). Nitrogen compounds are, besides sulfur, well-known poisons of noble metal hydrogenation catalysts (2, 3). Previously, it has been shown that the high specific hydrogenation rate of the Pt/USY sample (Table 5) could be associated to the formation of electron-deficient Pt species promoted by the electron withdrawing effect that the strong Brönsted acid sites present in the zeolite induced on the small Pt clusters inside the zeolite cavities. Then, the electron-donating nitrogen compounds present in the hydrotreated LCO feed may strongly adsorb on the electron-deficient Pt species in Pt/USY, reducing their hydrogenation activity. On the other hand, the nitrogen compounds may also interact with the strong Brönsted acid sites, decreasing the acidity of the zeolite (44), and consequently reducing the number of the highly active electron-deficient Pt particles in the catalyst.

CONCLUSIONS

It has been shown that MCM-41 materials having very high surface area and a regular arrangement of uniform mesopores are excellent supports for preparing highly disperse Pt-supported catalysts. These catalysts showed, together with the mesoporous amorphous silica-alumina (MSA), a superior activity for the hydrogenation of naphthalene than other conventional Pt-containing supports, such as commercial amorphous silica-alumina, silica, γ-alumina, and zeolite USY at moderate temperatures. However, the turnover number (activity per surface exposed Pt) was seen to be higher for the zeolite-based catalyst, despite its lower metal dispersion. This is explained by an important contribution of small Pt clusters localized in the supercages of the zeolite, which are subjected to a higher interaction with the strong Brönsted acid sites of the zeolite to form electron-deficient Pt particles of enhanced hydrogenation activity and improved sulfur tolerance.

Indeed, when a naphthalene feed containing of 200 ppm sulfur added as dibenzothiophene (DBT) was used, both the Al-containing MCM-41 and USY supports showed the higher sulfur resistance among the catalysts studied. The high metal dispersion and the interaction of the small Pt clusters (10–15 Å mean particle size) with the Brönsted acid sites of mild acidity present in Al-MCM-41 may account for the high sulfur tolerance of this catalyst.

Furthermore, Pt/(Al)MCM-41 also presented the highest activity for hydrogenation of aromatics in a hydrotreated light cycle oil (LCO) feedstock containing 400 ppm sulfur,

especially at the lowest temperature studied (300°C), further confirming the excellent properties of the mesoporous MCM-41 material as a support for preparing noble metal-based hydrogenation catalysts.

ACKNOWLEDGMENTS

Financial support by the Dirección General de Investigación Científica y Técnica of Spain (Project MAT 94-0166) is gratefully acknowledged. The authors also thank the Centro de Investigación of CEPSA (Madrid, Spain) and Eniricerche (Milan, Italy) for the analytical support given. V.M. acknowledges financial support from the Generalitat Valenciana.

REFERENCES

1. van den Berg, J. P., Lucien, J. P., Germaine, G., and Thielemans, G. L. B., *Fuel Process. Technol.* **35**, 119 (1993).
2. Stanislaus, A., and Cooper, B. H., *Catal. Rev. Sci. Eng.* **36**(1), 75 (1994).
3. Cooper, B. H., and Donnis, B. B. L., *Appl. Catal. A* **137**, 203 (1996).
4. Cooper, B. H., Stanislaus, A., and Hannerup, P. N., *Hydroc. Process.* **June**, 83 (1993).
5. Unzelman, G. H., "NPRA Annual Meeting, Paper AM-87-33, March 1987."
6. *Oil Gas J.* **Aug. 17**, 88 (1992).
7. Cooper, B. H., Stanislaus, A., and Hannerup, P. N., ACS Prepr., Div. of Fuel Chem. **37**(1), 41 (1992).
8. Barbier, J., Lamy-Pitara, E., Marecot, P., Boitiaux, J. P., Cosyns, J., and Verna, F., *Adv. Catal.* **37**, 279 (1990).
9. Arcoya, A., Cortés, A., Fierro, J. L. G., and Seoane, X. L., *Stud. Surf. Sci. Catal.* **68**, 557 (1991).
10. Lin, S. D., and Vannice, M. A., *J. Catal.* **143**, 539 (1993).
11. Lin, S.D., and Vannice, M. A., *J. Catal.* **143**, 554 (1993).
12. Koussathana, M., Vamvouka, D., Economon, H., and Verykios, X., *Appl. Catal.* **77**, 283 (1991).
13. Koussathana, M., Vanivouka, N., Tsapatsis, M., and Verykios, X., *Appl. Catal. A* **80**, 99 (1992).
14. Seoane, X. L., L'Argentiere, P. C., Fígoli, N. S., and Arcoya, A., *Catal. Lett.* **16**, 137 (1992).
15. Marécot, P., Mahoungon, J. R., and Barbier, J., *Appl. Catal. A* **101**, 143 (1993).
16. Corma, A., Martínez, A., Martínez-Soria, V., and Montón, J. B., *J. Catal.* **153**, 25 (1995).
17. Kresge, C. T., Leonowicz, M. E., Roth, W. J., Vashuli, J. C., and Beck, J. S., *Nature* **October**, 359 (1992).
18. Armor, J. N., *Appl. Catal.* **112**, N21 (1994).
19. Heinerman, J., and Vogt, E., PCT Int. Pat Appl. WO 94/26846 (1994).
20. Reddy, K. M., and Song, C., *Catal. Lett.* **36**, 103 (1996).
21. Reddy, K. M., and Song, C., *Catal. Today* **31**, 137 (1996).
22. Reddy, K. M., and Song, C., Prepr. ACS, Div. Fuel Chem. **46**(3), 906 (1996).
23. Bellussi, G., Perego, C., Carati, A., Peratello, S., Massana, C. P., and Perego, G., *Stud. Surf. Sci. Catal.* **84**, 85 (1994).
24. Beck, J. C., Chu, C., Jhonson, Z. D., Kresge, C. T., Leonowicz, M. E., Roth, W. J., and Vashuli, J. C., World Pat. WO 91/11390 (1991).
25. Corma, A., Fornés, V., Martínez, A., and Orchillés, A. V., ACS Symp. Ser. **368**, 542 (1988).
26. Corma, A., Grande, M. S., Gonzalez-Alfaro, V., and Orchillés, A. V., *J. Catal.* **159**, 375 (1996).
27. Mokaya, R., Jones, W., Luan, Z., Alba, M. D., and Klinowski, J., *Catal. Lett.* **37**, 113 (1996).
28. Lin, S. D., and Song, C., *Catal. Today* **31**, 93 (1996).
29. Girgis, M. J., and Gates, B. C., *Ind. Eng. Chem. Res.* **30**, 2021 (1991).
30. Frye, C. G., and Weitkamp, A. W., *J. Chem. Eng. Data* **14**, 372 (1969).
31. Bouchy, M., Peureux-Denys, S., Dufresne, P., and Kasztelan, S., *Ind. Eng. Chem. Res.* **32**, 1592 (1992).
32. Zhan, X. D., and Guin, J. A., *Energy & Fuels* **8**(6), 1384 (1994).
33. Smittz, A. D., Bowers, G., and Song, C., *Catal. Today* **31**, 45 (1996).
34. Lewis, P. H., *J. Catal.* **11**, 162 (1968).
35. Dalla Betta, R. A., and Boudart, M., "Proc. 5th Int. Congress on Catal.," Vol. 2, p. 1329. North Holland, 1973.
36. Gallezot, P., Datka, J., Massardier, J., Primat, M., and Imelik, B., "Proc. 6th Int. Congress on Catal.," Vol. 2, p. 696. The Chemical Society, London, 1977.
37. Kokayeff, P., "Catalyst Hydroprocessing of Petroleum and Distillates," p. 253. Dekker, New York, 1994.
38. Chou, P., and Vannice, M.A., *J. Catal.* **107**, 129 (1987).
39. Chou, P., and Vannice, M. A., *J. Catal.* **107**, 140 (1987).
40. Gallezot, P., and Bergeret, G., "Catalyst Deactivation" (E. E. Peterson and A. T. Bell, Eds.), p. 263. Dekker, New York, 1987.
41. Schatler, W. M. H., and Yu Stakheev, A., *Catal. Today* **12**, 283 (1992).
42. Dalla Betta, R. A., Boudart, M., Gallezot, P., and Weber, R. S., *J. Catal.* **69**, 514 (1981).
43. Homeyer, S. T., and Schatler, W. M. H., *Stud. Surf. Sci. Catal.* **49**, 975 (1989).
44. Dufresne, P., Quesada, A., and Miguard, S., *Stud. Surf. Sci. Catal.* **53**, 301 (1990).
45. Horvath, G., and Kawazoe, K. J., *Chem. Eng. Japan* **16**, 470 (1983).
46. Emeis, C. A., *J. Catal.* **141**, 347 (1993).